

Critical role of prostate apoptosis response-4 in determining the sensitivity of pancreatic cancer cells to small-molecule inhibitor-induced apoptosis

Asfar Sohail Azmi,¹ Zhiwei Wang,¹
Ravshan Burikhanov,³ Vivek M. Rangnekar,³
Guoping Wang,⁴ Jianyong Chen,⁴
Shaomeng Wang,⁴ Fazlul H. Sarkar,¹
and Ramzi M. Mohammad^{1,2}

¹Department of Pathology and ²Department of Internal Medicine, Division of Hematology/Oncology, Wayne State University School of Medicine, Karmanos Cancer Institute, Detroit, Michigan; ³Department of Radiation Medicine, University of Kentucky, Lexington, Kentucky; and ⁴University of Michigan, Ann Arbor, Michigan

Abstract

Role of prostate apoptosis response-4 (PAR-4) has been well described in prostate cancer. However, its significance in other cancers has not been fully elucidated. For the current study, we selected four pancreatic cancer cell lines (BxPC-3, Colo-357, L3.6pl, and HPAC) that showed differential endogenous expression of PAR-4. We found that nonpeptidic small-molecule inhibitors (SMI) of Bcl-2 family proteins (apogossypolone and TW-37; 250 nmol/L and 1 μ mol/L, respectively) could induce PAR-4-dependent inhibition of cell growth and induction of apoptosis. Sensitivity to apoptosis was directly related to the expression levels of PAR-4 ($R = 0.92$ and $R^2 = 0.95$). Conversely, small interfering RNA against PAR-4 blocked apoptosis, confirming that PAR-4 is a key player in the apoptotic process. PAR-4 nuclear localization is considered a prerequisite for cells to undergo apoptosis, and we found that the treatment of Colo-357 and L3.6pl cells with 250 nmol/L SMI leads to nuclear localization of PAR-4 as confirmed by 4',6-diamidino-2-phenylindole staining. In combination studies with gemcitabine, pretreatment with SMI leads to sensitization of Colo-357 cells to the growth-inhibitory and apoptotic action of a therapeutic drug,

gemcitabine. In an *in vivo* setting, the maximum tolerated dose of TW-37 in xenograft of severe combined immunodeficient mice (40 mg/kg for three i.v. injections) led to significant tumor inhibition. Our results suggest that the observed antitumor activity of SMIs is mediated through a novel pathway involving induction of PAR-4. To our knowledge, this is the first study reporting SMI-mediated apoptosis involving PAR-4 in pancreatic cancer. [Mol Cancer Ther 2008;7(9):2884–93]

Introduction

Last year 33,730 Americans were diagnosed with pancreatic cancer and 32,300 died from it, making pancreatic cancer the fourth leading cause of cancer death (1). It was estimated that worldwide 213,000 people will die from pancreatic cancer (2). These numbers will only grow as the population ages. Pancreatic cancer is an exceptionally devastating and incurable disease, the treatment of which has largely been unsuccessful due in part to the higher resistance of pancreatic tumor cells to conventional therapies. Therefore, there is a need for the development of new and effective therapy, which can target multiple signaling pathways to induce responsiveness of pancreatic cancer cells to death signals.

Prostate apoptosis response-4 (PAR-4), the product of the proapoptotic gene *Par-4*, was first identified in prostate cancer cells that were induced to undergo apoptosis (3). PAR-4 is a leucine zipper domain protein that is widely expressed in diverse normal and cancerous cell types and tissues (4, 5). Endogenous PAR-4 itself does not cause apoptosis, yet it is essential for apoptosis induced by a variety of exogenous insults (4, 5). It has been reported that ectopic PAR-4 overexpression is sufficient to induce apoptosis in most cancer cells but not in normal or immortalized cells (6). Cancer cells that are resistant to nuclear translocation of PAR-4 are resistant to apoptosis by PAR-4 (5, 7). Studies have also revealed that nuclear translocation of PAR-4 is essential for inhibition of pro-cell survival nuclear factor- κ B activity (5–8) and this apoptotic action is not inhibited by Bcl-2 or Bcl-X_L overexpression (5, 6). In view of its cancer cell-specific apoptotic property, PAR-4 becomes an interesting candidate target for exploiting novel therapeutic strategies for pancreatic cancer.

Our laboratory has recently been interested in the development of anticancer strategies using small-molecule inhibitors (SMI) of Bcl-2 family proteins (9, 10). Apogossypolone (ApoG2) is an analogue of gossypol, whereas *N*-[(2-tert-butyl-benzenesulfonyl)-phenyl]-2,3,4-trihydroxy-5-(2-isopropyl-benzyl)-benzamide (TW-37), a recently developed SMI of Bcl-2 that targets multiple members of the Bcl-2 family, appears to attenuate Bcl-2 activation (11, 12).

Received 5/5/08; revised 6/20/08; accepted 6/21/08.

Grant support: National Cancer Institute, NIH grant R01CA109389 (R.M. Mohammad) and NIH grant P30 CA22453-20 (S. Wang).

The costs of publication of this article were defrayed in part by the payment of page charges. This article must therefore be hereby marked *advertisement* in accordance with 18 U.S.C. Section 1734 solely to indicate this fact.

Requests for reprints: Ramzi M. Mohammad, Department of Internal Medicine, Division of Hematology/Oncology, Wayne State University School of Medicine, Karmanos Cancer Institute, 732 HWCRC, 4100 John R Street, Detroit, MI 48201. Phone: 313-576-8329; Fax: 313-576-8389. E-mail: Mohammad@karmanos.org

Copyright © 2008 American Association for Cancer Research.

doi:10.1158/1535-7163.MCT-08-0438

We have found that both ApoG2 and TW-37 inhibits the growth of a variety of cancer cells, including breast, prostate, and lymphoma *in vitro* and tumor growth *in vivo* and are nontoxic to normal cells such as human peripheral lymphocytes (10–12). Although there has been rapid progress for elucidating the mechanism of action of TW-37 as an antitumor agent, the exact mechanism has not yet been fully established.

Although pancreatic cancer show some response to gemcitabine therapy, most patients are either resistant at the beginning of the treatment or acquire resistance during therapy, a feature that essentially characterizes this fatal disease (13–16). Thus, we have also tested whether SMI-induced activation of PAR-4 could sensitize cells to gemcitabine to undergo apoptosis, and our results clearly show that SMI treatment of pancreatic cancer cells leads to sensitization of cells to gemcitabine-induced killing.

Materials and Methods

Cell Culture and Experimental Reagents

Human pancreatic cancer cell lines BxPC-3, Colo-357, HPAC, and L3.6pl were used in this study. BxPC-3 and HPAC (American Type Culture Collection) were cultured in RPMI 1640 (Invitrogen) supplemented with 10% fetal bovine serum and 1% penicillin and streptomycin. Colo-357 and L3.6pl cells were generously provided by Dr. Paul Chiao (M. D. Anderson Cancer Center) and grown as a monolayer cell culture in DMEM containing 4.5 mg/mL D-glucose and L-glutamine supplemented with 10% fetal bovine serum.

All cells were cultured in a 5% CO₂ humidified atmosphere at 37°C. Primary antibody for PAR-4 was purchased from Santa Cruz Biotechnology. All secondary antibodies were obtained from Pierce. LipofectAMINE 2000 was purchased from Invitrogen. Chemiluminescence detection of proteins was done with the use of a kit from Amersham Biosciences (Amersham Pharmacia Biotech). Protease inhibitor cocktail and all other chemicals were obtained from Sigma. The small interfering RNA (siRNA) oligonucleotide duplexes for human and mouse PAR-4 were from Santa Cruz Biotechnology. Human and mouse PAR-4 show >85% similarity at the amino acid level. Importantly, all critical domains, especially those involved in the induction of apoptosis, are conserved in human and mouse PAR-4. The human PAR-4 siRNA sequence targets human PAR-4 RNA at an area that shows maximal divergence from mouse PAR-4; accordingly, only 11 of 19 nucleotides are similar in human and mouse PAR-4 siRNA. The human PAR-4 siRNA inhibits human PAR-4, whereas the mouse PAR-4 siRNA does not inhibit human PAR-4 as confirmed by previous studies (7). Therefore, mouse PAR-4 siRNA was used as a control in the studies done in L3.6pl and Colo-357 cells.

TW-37

Design, synthesis, purification, and chemical characterization of TW-37 have been described in detail previously by Wang et al. (17).

Western Blot Analysis

Cells were lysed in lysis buffer [50 mmol/L Tris (pH 7.5), 100 mmol/L NaCl, 1 mmol/L EDTA, 0.5% NP-40, 0.5% Triton X-100, 2.5 mmol/L sodium orthovanadate, 10 µL/mL protease inhibitor cocktail, and 1 mmol/L phenylmethylsulfonyl fluoride] by incubating for 20 min at 4°C. The protein concentration was determined using the Bio-Rad assay system. Total proteins were fractionated using SDS-PAGE and transferred onto a nitrocellulose membrane for Western blotting as described earlier (18). Primary antibodies were anti-PAR-4 at 1:1,000 (Santa Cruz Biotechnology) and anti-actin at 1:5,000 (A5441; Sigma). Appropriate secondary horseradish peroxidase-linked antibodies (Amersham or Bio-Rad) were used. Membranes were developed with SuperSignal chemiluminescence (Pierce) and images captured on film, scanned as Adobe files, and formatted in PowerPoint. Densitometry was done on a Gel Doc 1000 (Bio-Rad), and signals were normalized to actin expression. Values from at least three different gels from two or more independent experiments were included in the analysis.

For testing effects of ApoG2 on protein expression, Colo-357 and L-3.6pl cells were cultured to subconfluence. On day 0, medium was exchanged to include ApoG2 at the final concentration of 0 (DMSO control), 250, and 1 µmol/L. Total cell extract was harvested 24, 48, and 72 h later and probed and analyzed as above.

Cell Growth Inhibition by Trypan Blue and 3-(4,5-Dimethylthiazol-2-yl)-2,5-Diphenyltetrazolium Bromide Assay

BxPC-3, Colo-357, L3.6pl, and HPAC cells were seeded at a density of 3×10^3 per well in 96-well microtiter culture plates. After overnight incubation, medium was removed and replaced with fresh medium containing different concentrations of ApoG2 (0.5–2 µmol/L) diluted from a 10 mmol/L stock. On completion of incubation, viability was assessed after adding 50 µL trypan blue solution (0.4% in PBS) in culture medium. After 1 to 2 min, the number of dead cells, which retained the dye, was compared with the total number to calculate the percentage of viable cells. Cell growth inhibition was also detected using 3-(4,5-dimethylthiazol-2-yl)-2,5-diphenyltetrazolium bromide (MTT) assay. Colo-357 and L3.6pl cells were exposed to different concentrations of SMI either alone or in combination with gemcitabine in 96-well microtiter plate. After the incubation, 20 µL MTT dye was added (5 mg/mL in PBS) to each well and the plates were incubated further for 2 h. On termination, the supernatant was aspirated and the MTT formazan formed by metabolically viable cells was dissolved in 100 µL isopropanol. The plates were gently rocked for 30 min on a gyratory shaker, and absorbance was measured at 595 nm using ULTRA Multifunctional Microplate Reader (TECAN).

Apoptosis Assay

Nucleosomal DNA was assayed with the ELISA^{PLUS} (Roche) kit using the protocol provided by the manufacturer with minor modifications. Colo-357 and L3.6pl cells were plated in duplicate wells at 2.0×10^5 per well in

six-well dishes and cultured overnight. ApoG2 was added at 0 to 2 $\mu\text{mol/L}$. At 24, 48, and 72 h, both floating and trypsinized cells were collected and washed, and both viable and dead cells were counted by trypan staining. In another set of experiments, Colo-357 cells were treated with TW-37 (250 nmol/L) either alone or in combination with gemcitabine (25 or 50 nmol/L). Fifty thousand cells (live or dead) were extracted with 500 μL incubation buffer, and after centrifugation, the supernatant was saved at -20°C . A sample of 100 μL of each extract (diluted 1:10 in incubation buffer) was processed per protocol. Signal was assayed for absorption at 405 nm in the Ultra plate reader. The mean and SD from at least two independent experiments (n of at least 4) were plotted with Prism software.

siRNA Transfections

Colo-357 and L3.6pl cells were transfected with PAR-4 siRNA and control siRNA, respectively, using LipofectAMINE 2000 Plus reagents. The transfected cells were treated with 250 or 1 $\mu\text{mol/L}$ ApoG2 for 72 h or kept as control. The proteins were extracted and measured by Western blot. In addition, apoptosis in transfected cells with treatments was detected using 4',6-diamidino-2-phenylindole (DAPI) staining and histone/DNA ELISA assay.

DAPI Staining

For protein localization, cells were grown on glass chamber slides and fixed with 10% paraformaldehyde for 20 min. Cells were incubated on ice for 30 min in solution of 100 μg DAPI in 100 mL PBS. The slides were dried and mounting medium was added to it and covered with a coverslip. A total of three independent experiments were done; in each experiment, 200 cells were scored for apoptosis under a confocal microscope. The cells are scored

for apoptosis depending on nuclear morphology as described previously (5).

Colo-357 Xenografts

Four-week-old female ICR-SCID mice were obtained from Taconic Laboratory. The mice were adapted to animal housing and Colo-357 xenografts were developed as described earlier (19). Briefly, three mice received 10^7 Colo-357 cells (in serum-free RPMI 1640) s.c. in each flank area. When s.c. tumors developed to about 1,500 mg, the tumors were excised, and serial propagation was accomplished by trimming extraneous material, cutting the tumors into fragments of 20 to 30 mg, which were then transplanted s.c. using a 12-gauge trocar into the flanks of a new group of mice for maintenance of tumors as well as for experimental purpose. For the subsequent drug efficacy trials, small fragments of the Colo-357 xenograft were implanted s.c. and bilaterally into naive, similarly adapted mice. Mice were checked three times per week for tumor development. Once transplanted, Colo-357 fragments developed into palpable tumors (60-100 mg); animals were removed randomly and assigned to different treatment groups. Using this model, the efficacy of TW-37 was studied. The maximum tolerated dose of TW-37 in severe combined immunodeficient mice was determined previously by our laboratory (20). Mice were injected with TW-37 at 20 mg/kg i.v., 3 consecutive days per week, for 2 weeks. Mice in the control and TW-37-treated group were followed for measurement of s.c. tumors, changes in body weight, and side effects of the drugs. Tumors were measured two times per week. Tumor weight (mg) was calculated using the formula: $(A \times B^2) / 2$, where A and B are the tumor length and width (mm). To avoid discomfort in the control group, animals were euthanized when their total tumor burden reached 2,000 mg. All studies involving

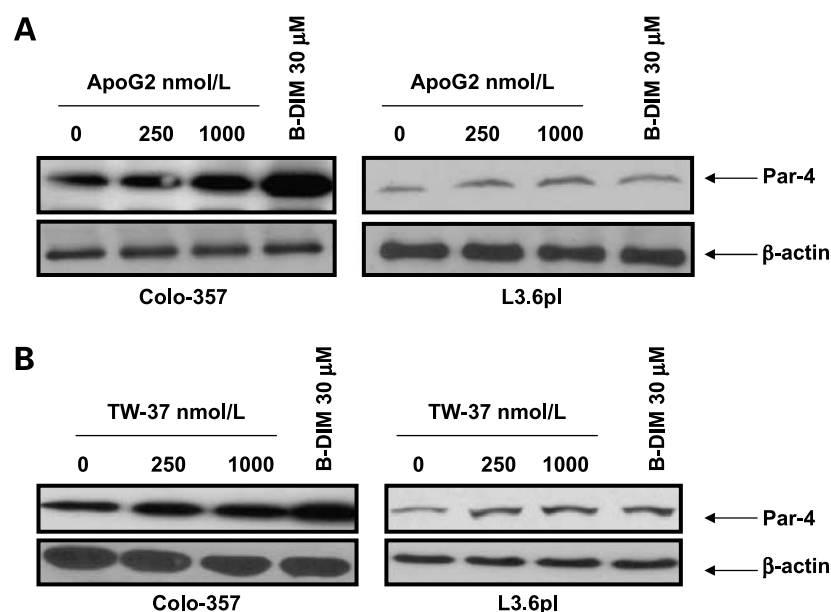


Figure 1. PAR-4 expression is up-regulated by ApoG2 and TW-37. **A, left,** Western blot analysis of lysates of Colo-357 cells treated with DMSO (untreated; lane 1); 250 nmol/L ApoG2 (lane 2); 1 $\mu\text{mol/L}$ ApoG2 (lane 3); 30 $\mu\text{mol/L}$ B-DIM (+ve control; lane 4), respectively. **Right panel,** Western blot analysis of lysates of L3.6pl cells treated with DMSO (untreated; lane 1); 250 nmol/L ApoG2 (lane 2) and 1 $\mu\text{mol/L}$ ApoG2 (lane 3); 30 $\mu\text{mol/L}$ B-DIM (+ve control; lane 4), respectively. **B, left,** Western blot analysis of lysates of Colo-357 cells treated with DMSO (untreated; lane 1); 250 nmol/L TW-37 (lane 2); 1 $\mu\text{mol/L}$ TW-37 (lane 3); 30 $\mu\text{mol/L}$ B-DIM (+ve control; lane 4), respectively. **Right panel,** Western blot analysis of lysates of L3.6pl cells treated with DMSO (untreated; lane 1); 250 nmol/L TW-37 (lane 2) and 1 $\mu\text{mol/L}$ TW-37 (lane 3); 30 $\mu\text{mol/L}$ B-DIM (+ve control; lane 4), respectively (right). β -Actin protein was used as loading control as shown for each blot.

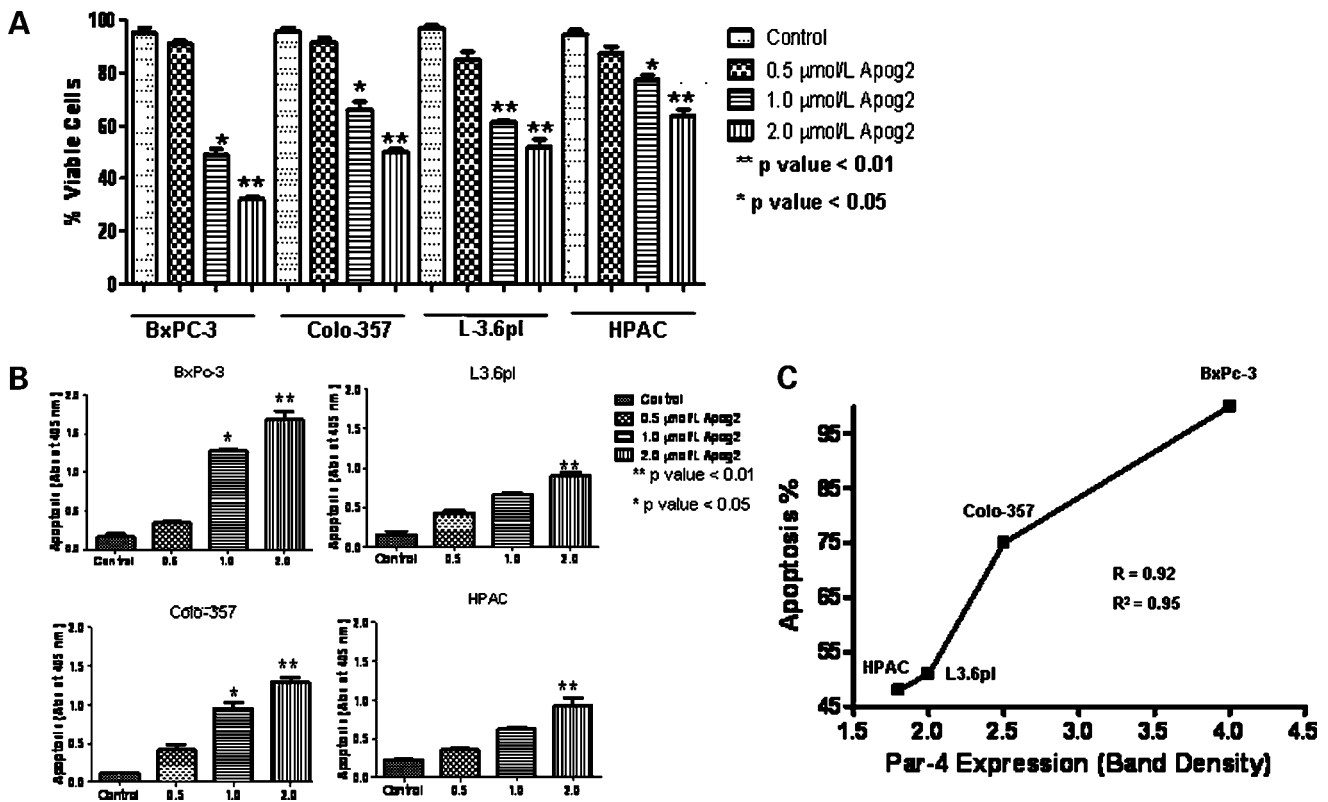


Figure 2. **A**, evaluation of cell viability in ApoG2-treated BxPC-3, Colo-357, L3.6pl, and HPAC cells by trypan blue staining. Cells were either untreated (DMSO) or treated with increasing concentration of ApoG2 (0.5–2 μmol/L) for 72 h and then analyzed for viable cells by trypan blue staining assay as described in Materials and Methods. The treatment of all pancreatic cancer cells with ApoG2 resulted in cell growth inhibition. The inhibition of cell growth was dose dependent. *, $P < 0.05$; **, $P < 0.01$, compared with untreated control. **B**, ApoG2-induced apoptosis in BxPC-3, L3.6pl, Colo-357, and HPAC pancreatic cancer cells was measured with the histone/DNA fragment analysis by using an ELISA. Control lane, control cells were treated with DMSO. Cells were treated with 0.5, 1, and 2 μmol/L ApoG2 for 72 h. *, $P < 0.05$; **, $P < 0.01$, compared with untreated control. **C**, apoptosis sensitivity is directly correlated to PAR-4 expression. % Apoptosis at maximum ApoG2 dose (2 μmol/L) calculated from values obtained from **B** are plotted on Y axis against densitometric values of PAR-4 from Fig. 1 X axis. R and R^2 values were calculated using GraphPad Prism software.

mice were done under Animal Investigation Committee-approved protocols.

Immunohistochemical Determination of PAR-4

The expression of PAR-4 was detected in histologic sections of tumor xenografts. Sections were cut from formalin-fixed, paraffin-embedded tissue blocks, collected on 3-ethoxy-aminoethyl-silane-treated slides, and allowed to dry overnight at 37°C. Sections were dewaxed in xylene, rehydrated through graded concentrations of ethanol to distilled water, immersed in 10 mmol/L citrate buffer (pH 6.0), and processed in a thermostatic water bath for 40 min at 98°C for antigen retrieval. Anti-PAR-4 (Santa Cruz Biotechnology); dilution 1:100 was applied on three slides for each case, and incubations were done overnight at room temperature in a humidified atmosphere followed by a 30-min incubation of secondary antibody. Slides were then incubated with streptavidin peroxidase and visualized using the 3,3'-diaminobenzidine chromogen (Lab Vision).

Statistical Analysis

Data are represented as mean \pm SD for the absolute values or percent of controls. The statistical significance

of differential findings between experimental groups and control was determined by Student's t test as implemented by Excel 2000 (Microsoft). P values < 0.05 were considered statistically significant. Isobologram analysis of the combination of gemcitabine and ApoG2 in L3.6pl-GR cells were calculated using Calcsyn software and combination index (CI) values were plotted. The simple correlation R and coefficient of correlation R^2 was calculated between apoptosis and PAR-4 expression using GraphPad Prism software.

Results

SMI ApoG2 and TW-37 Up-regulate the Expression of PAR-4 in Pancreatic Cancer Cells

First, we tested whether our SMIs could have any effect on the expression of PAR-4 in cells having low basal levels of the proapoptotic protein PAR-4. Exposure of L3.6pl and Colo-357 cells to ApoG2 and TW-37 for 72 h resulted in a significant induction of PAR-4. The results are presented in Fig. 1, which confirms that the treatment of Colo-357 and L3.6pl cells with 250 and 1 μmol/L ApoG2 or TW-37

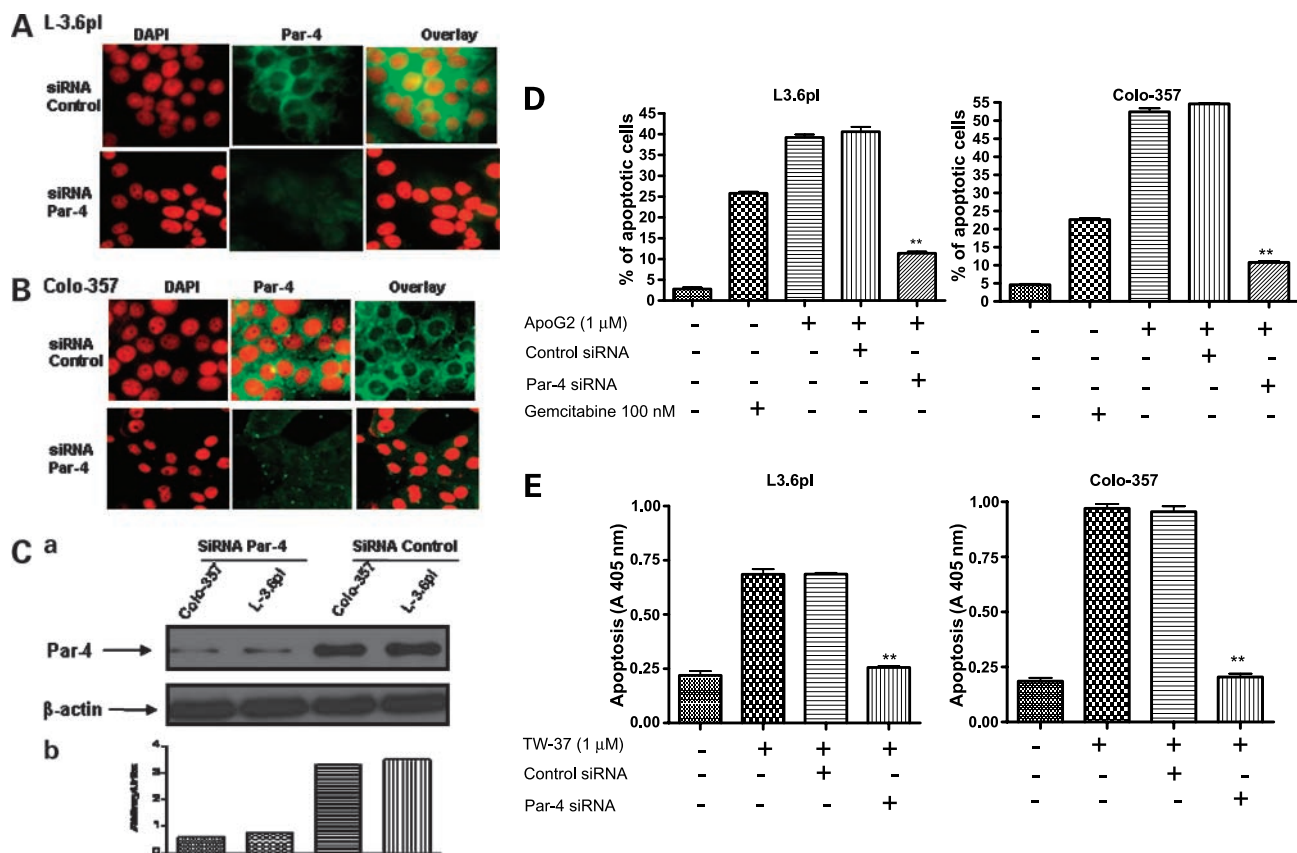


Figure 3. siRNA against PAR-4 inhibits apoptosis by SMI. **A**, L3.6pl and Colo-357 cells were transfected with the indicated constructs. The nuclei were stained with DAPI and visualized for localization of PAR-4 by confocal microscopy, and the transfectants were scored for apoptosis. Confocal microscopy images showing siRNA knockdown of PAR-4 in L3.6pl (**A**) and Colo-357 (**B**) cells. **C**, Western blot analysis of lysate extracted from siRNA-transfected L3.6pl and Colo-357 cells. Lane 1, Colo-357 + siRNA PAR-4; lane 2, L3.6pl + siRNA PAR-4; lane 3, Colo-357 + control siRNA; lane 4, L3.6pl + control siRNA. β -Actin protein was used as loading control as shown for the blot. Densitometric analysis of PAR-4 is shown in untreated, control siRNA-treated, and PAR-4-treated cells (*bottom*). The densitometric values were calculated as PAR-4/ β -actin ratios. Cell extracts were prepared according to the procedure described in Materials and Methods. **D**, apoptosis induction by ApoG2 in L3.6pl and Colo-357 cells with or without siRNA transfection. Cells were stained with DAPI and scored for apoptosis under fluorescent microscope. Bars, SD. **, $P < 0.001$, statistically significant compared with 1.0 μ mol/L ApoG2-treated control (Student's t test). **E**, DNA histone/ELISA apoptosis assay of PAR-4 siRNA-transfected L3.6pl and Colo-357 cells treated with (1 μ mol/L) TW-37. Bars, SD. **, $P < 0.001$, statistically significant compared with treated control (Student's t test).

induces PAR-4, which indeed may result in inhibition of cell growth and induction of apoptosis. In our earlier publication, we have shown that B-DIM, a chemopreventive agent, is able to induce PAR-4; therefore, it was used as a positive control (21).

Effect of ApoG2 on Cell Growth Inhibition and Apoptosis

To test the effect of ApoG2 on cell growth, four pancreatic cancer cell lines (BxPC-3, Colo-357, L3.6pl, and HPAC) were treated with increasing concentrations of ApoG2 (0–2 μ mol/L) for 72 h. As shown in Fig. 2A, cell growth was inhibited by ApoG2 treatment in a dose-dependent manner. In BxPC-3 cells, treatment with 0.5, 1, and 2 μ mol/L ApoG2 for 72 h resulted in 5%, 51%, and 73% inhibition of cell growth relative to control, respectively. Similarly, treatment of Colo-357 cells resulted in 4%, 31%, and 47% inhibition of cell growth, respectively, relative to control. In case of L3.6pl cells, ApoG2 treatment resulted

in 8%, 36%, and 42% growth inhibition, whereas for HPAC ApoG2 treatment resulted in 6%, 17%, and 31% cell growth inhibition. To assess whether treatment of cells with SMIs could also induce apoptosis, histone/DNA ELISA assay was done to verify whether cell growth inhibition was in part due to apoptosis. As can be seen in Fig. 2B, exposure of BxPC-3, L3.6pl, Colo-357, and HPAC pancreatic cancer cell lines to ApoG2 leads to a progressive increase in apoptosis. These results are consistent with the inhibition of cell growth, suggesting that growth inhibition by ApoG2 is partly due to the induction of apoptotic cell death. To correlate the apoptosis sensitivity to PAR-4 levels in BxPC-3, L3.6pl, Colo-357, and HPAC cells, we plotted the apoptosis (at maximum tested dose 2.0 μ mol/L) versus densitometric values of PAR-4 obtained from Fig. 1. Interestingly, the apoptotic induction was found to be greater in cell lines having higher basal levels of PAR-4 with correlation $R = 0.92$ and $R^2 = 0.95$ (Fig. 2C). The results clearly

establish the link between PAR-4 expression levels and apoptosis.

siRNA Knockdown of PAR-4 Inhibits Apoptosis by ApoG2 and a New Generation SMI TW-37

To verify the mechanistic role of PAR-4 in cellular apoptosis by SMI, siRNA against PAR-4 was used. Only human PAR-4 siRNA (Santa Cruz Biotechnology) was able to suppress PAR-4 in Colo-357 and L3.6pl cells (Fig. 3A and B), whereas its mouse counterpart (Santa Cruz Biotechnology) was ineffective and therefore was used as control (Fig. 3A and B, *top*). The suppression of PAR-4 was confirmed through DAPI staining as well as Western blot analysis of cells treated with PAR-4 siRNA (Fig. 3A-C). Knocking down PAR-4 in L3.6pl and Colo-357 cells resulted in 67% and 80% inhibition of ApoG2-mediated apoptosis, respectively (Fig. 3D). We also tested a newly developed and less toxic SMI TW-37 for its action on pancreatic cells. In TW-37-treated L3.6pl and Colo-357 cells, siRNA against PAR-4 inhibited apoptosis by 65% and 76%, respectively (Fig. 3E). Results obtained from this study indicate the involvement of PAR-4 in the induction of apoptosis induced by SMIs ApoG2 and TW-37.

ApoG2 Mobilizes PAR-4, a Proapoptotic Protein, into the Nucleus

It is well recognized that the *Par-4* gene induced during the process of apoptosis needs nuclear translocation for apoptosis (5). To understand the molecular mechanism involved in ApoG2-mediated cell death, we further analyzed the PAR-4 localization in pancreatic cancer cells exposed to ApoG2 using DAPI staining. As can be seen from Fig. 4A and B, fluorescence images of L3.6pl and

Colo-357 cells show no nuclear localization of PAR-4 in DAPI- or PAR-4-stained slides, whereas the orange fluorescence in the overlay images clearly indicates nuclear localization of PAR-4 in both cells. These results firmly establish that SMI treatment translocated the proapoptotic protein to the nucleus; PAR-4 could participate in the regulation of apoptotic processes. Because the induction of PAR-4 by SMIs leads to cell death, we speculated that the killing of these cells could be enhanced by a conventional chemotherapeutic agent, gemcitabine, which is routinely used for the treatment of pancreatic cancer.

SMI Potentiates Cell Growth Inhibition and Apoptosis Induced by Gemcitabine

We assessed the effect of pretreatment with TW-37 followed by gemcitabine treatment on cell viability by MTT assay. For these studies, cells were pretreated with TW-37 (0.25 or 0.5 $\mu\text{mol/L}$) followed by treatment with two doses of gemcitabine (25 or 50 nmol/L) and viable cells were evaluated at 72 h after treatment using MTT assay. The dose used here was chosen based on a preliminary dose escalation study done by us before this experiment. We found that treatment of Colo-357 cells with TW-37 resulted in 8% and 40% loss of cell viability, whereas treatment with gemcitabine (25 or 50 nmol/L) alone for 72 h resulted in only 3% and 9% loss of viability, respectively. However, pretreatment with TW-37 0.25 $\mu\text{mol/L}$ for 24 h followed by 48 h treatment with 25 nmol/L gemcitabine resulted in 35% cell growth inhibition. For the 0.5 $\mu\text{mol/L}$ TW-37 pretreatment plus 50 nmol/L gemcitabine, the growth inhibition was 60% (Fig. 5A). Isobologram analysis revealed a synergistic combination between SMI

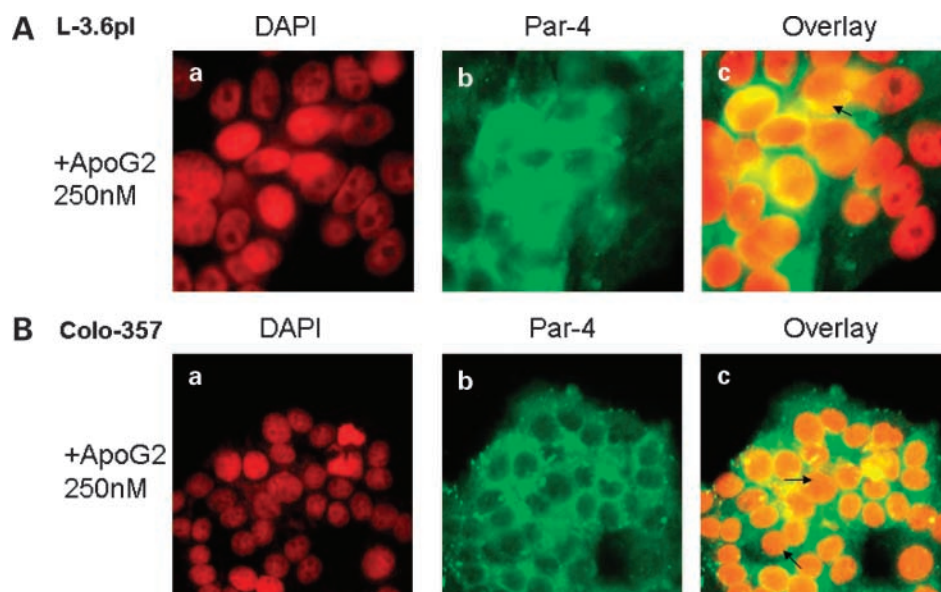


Figure 4. ApoG2 localizes PAR-4 into the nucleus of Colo-357 as well as L3.6pl cells. L3.6pl and Colo-357 cells were fixed and probed with PAR-4 antibody to detect expression of endogenous PAR-4. Nuclei were visualized by staining with DAPI. Intracellular localization of endogenous PAR-4 was recorded by confocal microscopy. **A** and **B**, L3.6pl and Colo-357 cells were exposed to ApoG2 (250 nmol/L) for 72 h and cells were stained with DAPI (pseudo-colored red) and visualized for localization of PAR-4 by confocal microscopy. **a**, DAPI stained; **b**, PAR-4 stained; **c**, overlay. Note orange fluorescence in overlay images confirms localization of PAR-4 in the nucleus on treatment with ApoG2.

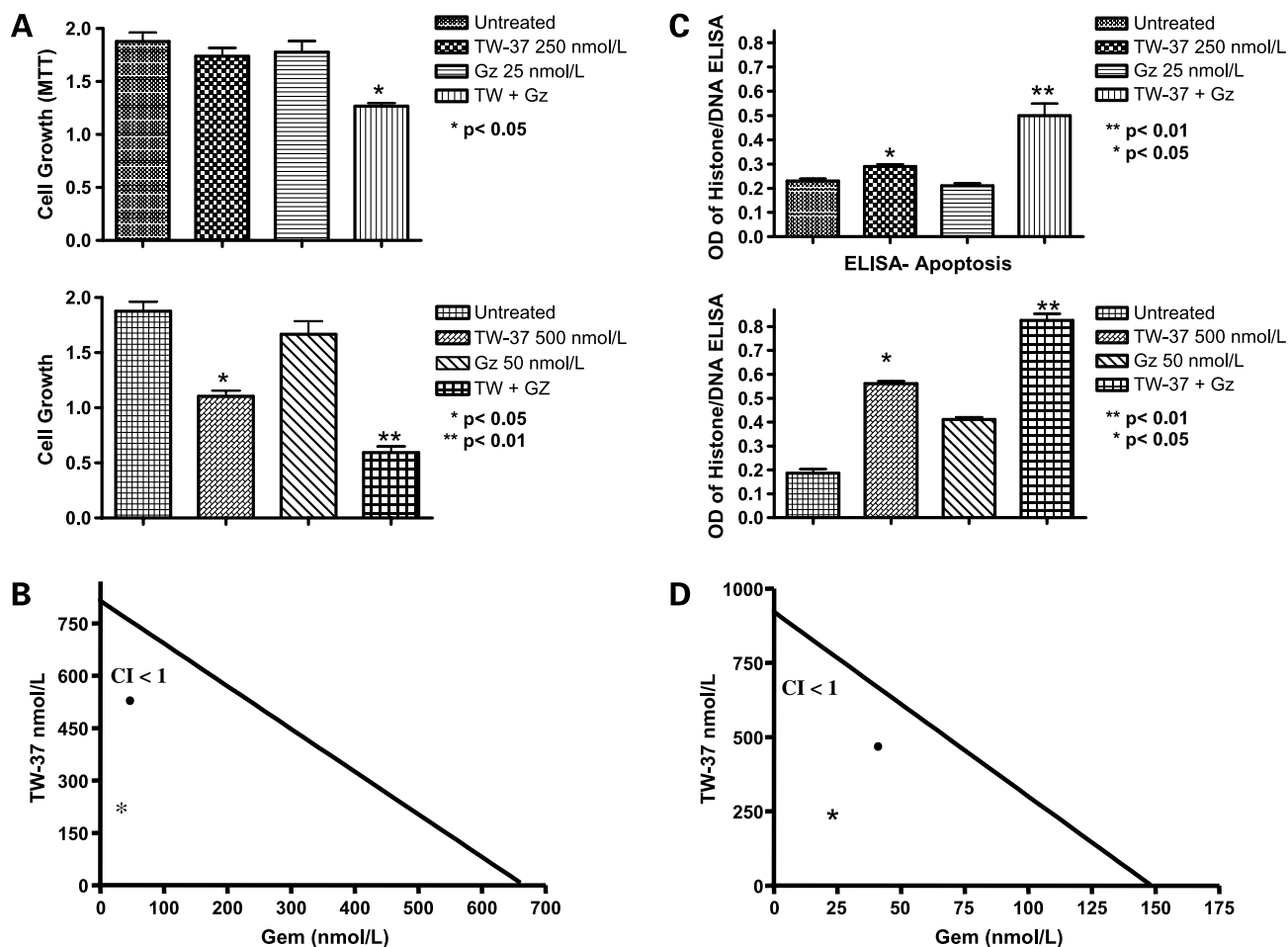


Figure 5. Sensitization Colo-357 cells by TW-37 to cytotoxic action of gemcitabine. **A**, TW-37 sensitizes Colo-357 cells to cytotoxic action of gemcitabine. Colo-357 cells were preincubated for 24 h with TW-37 followed by gemcitabine for 48 h. *Top panel*, 250 nmol/L TW-37 + 25 nmol/L gemcitabine; *bottom panel*, 500 nmol/L TW-37 + 50 nmol/L gemcitabine. Cell growth inhibition was determined using MTT assay. **B**, isobologram of *in vitro* drug combinations. Isobologram analysis of the combination of gemcitabine and TW-37 in Colo-357 cells (TW-37: gemcitabine 1:10 ratio). CI values were calculated using Calcsyn software. Points below the line indicate synergy. **C**, TW-37 sensitizes Colo-357 cells to apoptosis by gemcitabine. Colo-357 cells were preincubated for 24 h with TW-37 followed by gemcitabine treatment for 48 h. *Top panel*, 250 nmol/L TW-37 + 25 nmol/L gemcitabine and, *bottom panel*, 500 nmol/L TW-37 + 50 nmol/L gemcitabine. Apoptosis was detected using histone/DNA ELISA assay. **D**, isobologram of *in vitro* drug combinations. Isobologram analysis of the combination of gemcitabine and TW-37 in Colo-357 cells (TW-37: gemcitabine 1:10 ratio). CI values were calculated using Calcsyn software. Points below the line indicate synergy.

and gemcitabine with CI values < 1 (Fig. 5B). These results suggest that the pretreatment with low doses of TW-37 sensitizes the cells for better cell growth inhibition with conventional chemotherapeutic drug such as gemcitabine. We also did histone/DNA ELISA assay to verify whether TW-37 combines synergistically with gemcitabine to induce apoptosis. Although we observed minimal induction of apoptosis in Colo-357 with TW-37 (0.25 $\mu\text{mol/L}$ or 0.5 $\mu\text{mol/L}$) or gemcitabine (25 and 50 nmol/L) alone, relative to single agents, TW-37 pretreatment followed by gemcitabine treatment induced much more apoptosis in both cell lines as shown by histone DNA ELISA assay (Fig. 5C). In this case, the CI values were < 1, which is synergistic (Fig. 5D) and consistent with the results of cell growth inhibition observed by MTT assay. Collec-

tively, the above results clearly suggest that TW-37 sensitizes pancreatic cells to gemcitabine-induced killing; thus, further studies were done for initial testing whether TW-37 could show antitumor activity in a xenograft model.

Effect of TW-37 on Pancreatic Tumor Growth *In vivo*

To determine whether TW-37 could inhibit tumor growth in animals, we established Colo-357 human pancreatic cancer xenografts in severe combined immunodeficient mice (19). We found that mice in all treatment groups developed s.c. tumors. As shown in Fig. 6A, TW-37 treatment significantly inhibited tumor growth (images 3 and 4; $P = 0.015$ versus vehicle) compared with untreated control (images 1 and 2). We weighed the mice over 20 days of treatment using the same treatment dose of TW-37.

TW-37 did not show any toxicity or caused any loss in the body weight of the animals during the course of the treatment (up to 20 days). As can be seen in Fig. 6 (right), there is a significant decrease in tumor weight in TW-37 treated mice. We subsequently asked the question whether the antitumor activity of TW-37 could be correlated with the induction of PAR-4 as observed in our *in vitro* studies. An immunohistochemical analysis of tumor tissue stained with PAR-4 antibody revealed the presence of extensive necrosis in TW-37-treated tumors (Fig. 6B, right, black arrows). Further, compared with untreated control tumors, we observed higher staining of PAR-4 (Fig. 6B, right, white arrows). These results are consistent with our *in vitro* findings showing that the antitumor activity of SMI indeed involves activation of PAR-4.

Discussion

In recent years, SMIs of Bcl-2 family proteins have gained a lot of attention in the field of cancer research. Our laboratory and others have extensively studied several SMI (e.g., gossypol, ApoG2, and TW-37) for their anticancer and apoptosis-inducing properties in various cancers (9–12). The present study shows that SMIs ApoG2 and TW-37 induce apoptosis in pancreatic cancer cells and also inhibited tumor growth in a xenograft animal model. Our study shows the critical role of PAR-4 in determining the

sensitivity of pancreatic cancer cells as well as tumors to SMI-induced apoptosis.

One of the most promising aspects of SMIs in treating cancer is that their targets and mechanisms of action are different from those of cytotoxic drugs and radiation. This makes it feasible to combine SMIs with gemcitabine, creating a synergistic therapy, for pancreatic cancer without developing any cross-resistance or increased toxicity. In our opinion, both *de novo* and acquired resistance to therapy could be overcome by employing rational combination therapy, where toxic agents could be used in lower doses, but the efficacy of treatment could be increased by novel nontoxic agent that may have different mechanism of action. SMIs binds with high affinity to the hydrophobic groove found in the multidomain antiapoptotic Bcl-2 family proteins; this groove is naturally the site for interaction with BH3 α -helix in the BH3-only proapoptotic proteins. Drug binding is thought to block the antiapoptotic proteins from heterodimerizing with the proapoptotic members of the Bcl-2 family (Bad, Bid, and Bim) or may produce conformational changes that disable the antiapoptotic members. It has been proposed that the mechanism through which SMI inhibits Bcl-2 is that it interferes with the antiapoptotic and proapoptotic Bcl-2 family protein interaction rather than interfering with Bcl-2 family protein expression or stability; thus, we believe that the SMI disrupts the functional interaction of proteins but

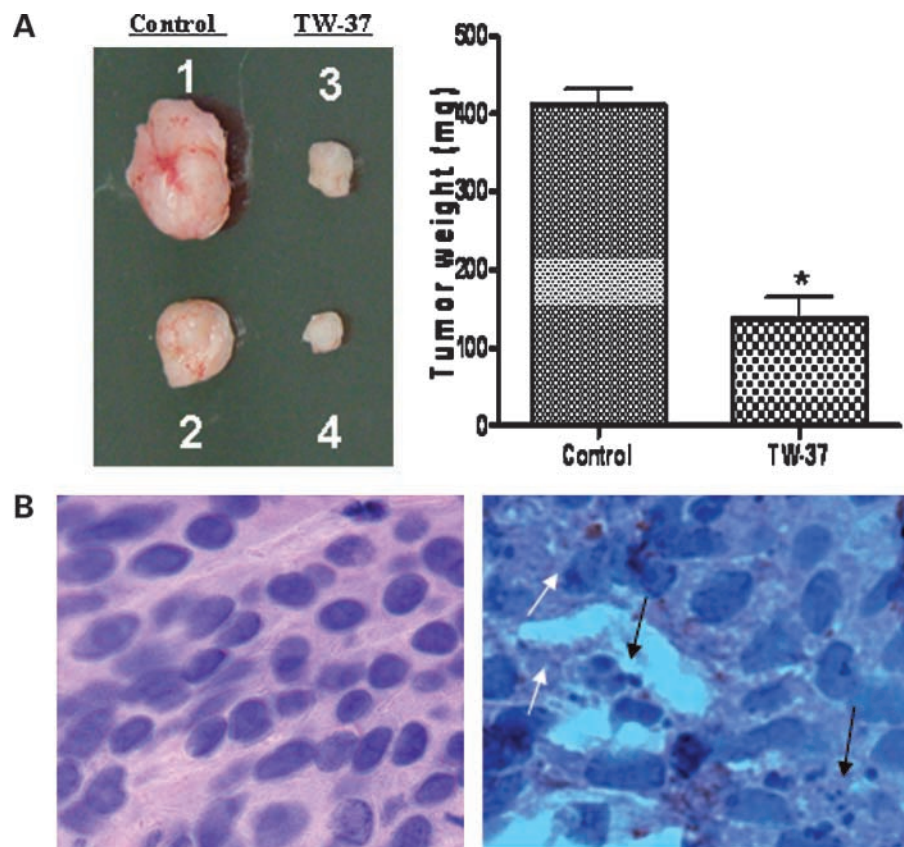


Figure 6. TW-37 inhibits tumor growth and induces PAR-4 expression in cancer tissue. Colo-357 xenografts were inoculated s.c. in severe combined immunodeficient mice. Once transplanted, fragments developed into palpable tumors (about 80 mg), and groups of nine animals were removed randomly and assigned to different treatment groups. Mice were injected with TW-37 at 20 mg/kg i.v. \times 3 d, for two cycles. The control group received vehicle only. **A**, TW-37 retards the growth of Colo-357 tumor xenografts in nude mice. **B**, PAR-4 staining of tumor tissue showing PAR-4 induction by TW-37-treated animal tumors. Control tumors (left) show insignificant PAR-4 staining. TW-37 treated tumors (right) show prominent PAR-4 staining (white arrows) as well as extensive necrosis (black arrows).

does not affect transcription of Bcl-2 family proteins (10). Therefore, we hypothesize that the activation of PAR-4 (an apoptosis-inducing molecule) by SMI could lead to sensitization of pancreatic cancer cells to conventional chemotherapeutic agent such as gemcitabine. Based on this rationale, we sought to assess the efficacy of ApoG2 and TW-37, two well-studied SMIs of Bcl-2 family proteins on four pancreatic cancer cell lines. In our study, we found that the treatment of different pancreatic cancer cell lines with low doses of ApoG2 (250 nmol/L to 1 μ mol/L) resulted in the induction of PAR-4 (Fig. 1). The induction of PAR-4 was directly correlated with inhibition of cell growth as tested by trypan blue exclusion assay (Fig. 2A) and induction of apoptosis as confirmed by histone/DNA ELISA and DAPI cell scoring (Figs. 2B and 3). Interestingly, sensitivity to apoptosis was directly correlated with PAR-4 expression in the four cell lines tested ($R = 0.92$ and $R^2 = 0.95$). Moreover, siRNA against PAR-4 abrogated apoptosis by SMI in L3.6pl and Colo-357 cells underscoring the critical role of PAR-4 in inducing apoptosis in pancreatic cancer cells. Further studies confirmed nuclear localization of PAR-4 as shown by DAPI staining of ApoG2-treated Colo-357 and L3.6pl cells (Fig. 4). Interestingly, nuclear localization of PAR-4 is considered a prerequisite for PAR-4-mediated apoptosis.

The nucleoside analogue gemcitabine remains the cornerstone of neoadjuvant and adjuvant chemotherapy in pancreatic cancer, although only a partial response is achieved in a minority of patients (13), thus resulting in a dismal progression-free survival interval ranging from 0.9 to 4.2 months (14, 15). However, many forms of pancreatic cancer show initial sensitivity to gemcitabine therapy followed by the rapid development of resistance, a feature that essentially characterizes this fatal disease. Overcoming the acquired resistance in pancreatic tumors through sensitization by novel agents such as SMI may be a promising new area of research. Interestingly, the combination of TW-37 with gemcitabine resulted in enhanced cell killing. Isobologram analysis of the data confirmed a synergistic mode of action between gemcitabine and TW-37, suggesting that further studies for this combination using multiple animal models of pancreatic cancer must be done in the future.

To identify the clinical relevance of our *in vitro* results, an initial pilot experiment was done using a xenograft animal model of pancreatic cancer. Immunohistochemical analysis of Colo-357 xenograft animal tissue stained with PAR-4 antibody revealed some interesting results. In the untreated control tumor tissues, we did not find any significant presence of PAR-4 and correspondingly negligible apoptosis or necrosis (Fig. 6B, *left*). In contrast, in the TW-37-treated tumors, we found extensive PAR-4 staining as well as high amount of necrotic cells (Fig. 6B, *right*). These observations provide evidence in support of the "proof-of-principle" for targeting PAR-4 by SMIs, which could be an important and new area in the treatment of pancreatic cancer. Nevertheless, based on a recent study using tissue array on multiple human normal as well as

tumor samples, it has been reported that the presence of PAR-4 is correlated with longer survival of patients with pancreatic cancer (22), suggesting that the presence of PAR-4 leads to enhanced killing of pancreatic cancer cells in patients during therapy.

In summary, we found that the SMIs ApoG2 and TW-37 induced cell growth inhibition and apoptosis in pancreatic cancer cells by modulating a novel gene product PAR-4. That the two SMIs could also sensitize pancreatic cancer cells to the cytotoxic action of gemcitabine underscores the importance of the SMIs for further development toward the treatment of pancreatic cancer by SMIs alone or in combination with conventional therapeutic agents.

Disclosure of Potential Conflicts of Interest

University of Michigan has filed a patent on TW-37, which has been licensed by Ascenta Therapeutics. University of Michigan and S. Wang own equity in Ascenta. S. Wang also serves as a consultant for Ascenta and is the principal investigator on a research contract from Ascenta to University of Michigan. The other authors reported no potential conflicts of interest.

References

- Jemal A, Siegel R, Ward E, Murray T, Xu J, Thun MJ. Cancer statistics. *CA Cancer J Clin* 2007;57:43–66.
- Jemal A, Siegel R, Ward E, Hao Y, Xu J, Murray T, Thun MJ. Cancer statistics. *CA Cancer J Clin* 2008;58:71–96.
- Sells SF, Wood DP Jr, Barve SSJ, et al. Commonality of the gene programs induced by effectors of apoptosis in androgen-dependent and -independent prostate cells. *Cell Growth Differ* 1994;5:457–66.
- Sells SF, Han S-S, Muthukkumar S, et al. Expression and function of the leucine zipper protein PAR-4 in apoptosis. *Mol Cell Biol* 1997;17:3823–32.
- El-Guendy N, Rangnekar VM. Apoptosis by PAR-4 in cancer and neurodegenerative diseases. *Exp Cell Res* 2003;283:51–66.
- El-Guendy N, Zhao Y, Gurumurthy S, Burikhanov R, Rangnekar VM. Identification of a unique core domain of PAR-4 sufficient for selective apoptosis-induction in cancer cells. *Mol Cell Biol* 2003;23:5516–25.
- Chakraborty M, Qiu SG, Vasudevan KM, Rangnekar VM. PAR-4 drives trafficking and activation of Fas and FasL to induce prostate cancer cell apoptosis and tumor regression. *Cancer Res* 2001;61:7255–63.
- Gurumurthy S, Goswami A, Vasudevan KM, Rangnekar VM. Phosphorylation of PAR-4 by protein kinase A is critical for apoptosis. *Mol Cell Biol* 2005;25:1146–61.
- Mohammad RM, Wang S, Banerjee S, Wu X, Chen J, Sarkar FH. Nonpeptidic small-molecule inhibitor of Bcl-2 and Bcl-XL, (-)-gossypol, enhances biological effect of genistein against BxPC-3 human pancreatic cancer cell line. *Pancreas* 2005;31:317–24.
- Arnold AA, Aboukameel A, Chen J, et al. Preclinical studies of Apogossypolone: a new nonpeptidic pan small-molecule inhibitor of Bcl-2, Bcl-XL and Mcl-1 proteins in follicular small cleaved cell lymphoma model. *Mol Cancer* 2008;7:20.
- Verhaegen M, Bauer JA, Martin dl V, et al. A novel BH3 mimetic reveals a mitogen-activated protein kinase-dependent mechanism of melanoma cell death controlled by p53 and reactive oxygen species. *Cancer Res* 2006;66:11348–59.
- Zeitlin BD, Joo E, Dong Z, et al. Antiangiogenic effect of TW37, a small-molecule inhibitor of Bcl-2. *Cancer Res* 2006;66:8698–706.
- Burris HA III, Moore MJ, Andersen J, et al. Improvements in survival and clinical benefit with gemcitabine as first-line therapy for patients with advanced pancreas cancer: a randomized trial. *J Clin Oncol* 1997;15:2403–13.
- Moore MJ, Hamm J, Dancey J, et al. Comparison of gemcitabine versus the matrix metalloproteinase inhibitor BAY 12-9566 in patients with advanced or metastatic adenocarcinoma of the pancreas: a phase III

trial of the National Cancer Institute of Canada Clinical Trials Group. *J Clin Oncol* 2003;21:3296–302.

15. Evans DB, Abbruzzese JL, Rich TZ. Cancer of the pancreas. In: DeVita VT, Hellman S, Rosenberg SA, editors. *Cancer, principles and practice of oncology*. 5th ed. Philadelphia: J.B. Lippincott Co.; 1997. p. 1054–87.

16. Schniewind B, Christgen M, Kurdow R, Haye S, Kremer B, Kalthoff H, Ungefroren H. Resistance of pancreatic cancer to gemcitabine treatment is dependent on mitochondria-mediated apoptosis. *Int J Cancer* 2004;109:182–8.

17. Wang G, Nikolovska-Coleska Z, Yang CY, et al. Structure-based design of potent small-molecule inhibitors of anti-apoptotic Bcl-2 proteins. *J Med Chem* 2006;49:6139–42.

18. Wang Z, Sengupta R, Banerjee S, et al. Epidermal growth factor receptor-related protein inhibits cell growth and invasion in pancreatic cancer. *Cancer Res* 2006;66:7653–60.

19. Mohammad RM, Dugan MC, Mohamed AN, et al. Establishment of a human pancreatic tumor xenograft model: potential application for preclinical evaluation of novel therapeutic agents. *Pancreas* 1998;16:19–25.

20. Mohammad RM, Goustin AS, Aboukameel A, et al. Preclinical studies of TW-37, a new nonpeptidic small-molecule inhibitor of Bcl-2, in diffuse large cell lymphoma xenograft model reveal drug action on both Bcl-2 and Mcl-1. *Clin Cancer Res* 2007;13:2226–35.

21. Azmi AS, Ahmad A, Banerjee S, Rangnekar VM, Mohammad RM, Sarkar FH. Chemoprevention of pancreatic cancer: characterization of PAR-4 and its modulation by 3,3'-diindolylmethane (DIM). *Pharm Res* 2008;25:2117–24.

22. Ahmed MM, Sheldon D, Fruitwala MA, et al. Downregulation of PAR-4, a pro-apoptotic gene, in pancreatic tumors harboring K-ras mutation. *Int J Cancer* 2008;122:63–70.

Molecular Cancer Therapeutics

Critical role of prostate apoptosis response-4 in determining the sensitivity of pancreatic cancer cells to small-molecule inhibitor-induced apoptosis

Asfar Sohail Azmi, Zhiwei Wang, Ravshan Burikhanov, et al.

Mol Cancer Ther 2008;7:2884-2893.

Updated version Access the most recent version of this article at:
<http://mct.aacrjournals.org/content/7/9/2884>

Cited articles This article cites 21 articles, 11 of which you can access for free at:
<http://mct.aacrjournals.org/content/7/9/2884.full#ref-list-1>

Citing articles This article has been cited by 1 HighWire-hosted articles. Access the articles at:
<http://mct.aacrjournals.org/content/7/9/2884.full#related-urls>

E-mail alerts [Sign up to receive free email-alerts](#) related to this article or journal.

Reprints and Subscriptions To order reprints of this article or to subscribe to the journal, contact the AACR Publications Department at pubs@aacr.org.

Permissions To request permission to re-use all or part of this article, use this link
<http://mct.aacrjournals.org/content/7/9/2884>.
Click on "Request Permissions" which will take you to the Copyright Clearance Center's (CCC) Rightslink site.